Dushaw BD, Worcester PF, Cornuelle BD and Howe BM (1993) On equations for the speed of sound in seawater. *Journal of the Acoustical Society of America* 93: 255–275.

Jensen FB, Kuperman WA, Porter MB and Schmidt H (1994) *Computational Ocean Acoustics*. Woodbury: AIP Press.

Keller and Papadakis JS (eds) (1977) *Wave Propagation in Underwater Acoustics*. New York: Springer-Verlag.

Makris NC, Chia SC and Fialkowski LT (1999) The biazimuthal scattering distribution of an abyssal hill. *Journal of the Acoustical Society of America* 106: 2491–2512.

Medwin H and Clay CS (1997) *Fundamentals of Acoustical Oceanography*. Boston: Academic Press.

Morris GB (1978) Depth dependence of ambient noise in the Northeastern Pacific Ocean. *Journal of the Acoustical Society of America* 64: 581–590.

Munk W, Worcester P and Wunsch C (1995) *Acoustic Tomography*. Cambridge: Cambridge University Press.

Nicholas M, Ogden PM and Erskine FT (1998) Improved empirical descriptions for acoustic surface backscatter in the ocean. *IEEE-JOE* 23: 81–95.

Northrup J and Colborn JG (1974) Sofar channel axial sound speed and depth in the Atlantic Ocean. *Journal of Geophysical Research* 79: 5633–5641.

Ross D (1976) *Mechanics of Underwater Noise*. New York: Pergamon.

Ogilvy JA (1987) Wave scattering from rough surfaces. *Reports on Progress in Physics* 50: 1553–1608.

Urick RJ (1979) *Sound Propagation in the Sea*. Washington, DC: US GPO.

Urick RJ (1983) *Principles of Underwater Sound*. New York: McGraw Hill.

Spiesberger JL and Metzger K (1991) A new algorithm for sound speed in seawater. *Journal of the Acoustical Society of America* 89: 2677–2688.

Wenz GM (1962) Acoustics ambient noise in the ocean: spectra and sources. *Journal of the Acoustical Society of America* 34: 1936–1956.

ACOUSTICS IN MARINE SEDIMENTS

T. Akal, NATO SACLANT Undersea Research Centre, La Spezia, Italy

doi:10.1006/rwos.2001.0316

Introduction

Because of the ease with which sound can be transmitted in sea water, acoustic techniques have provided a very powerful means for accumulating knowledge of the environment below the ocean surface. Consequently, the fields of underwater acoustics and marine seismology have both used sound (seismo-acoustic) waves for research purposes.

The ocean and its boundaries form a composite medium, which support the propagation of acoustic energy. In the course of this propagation there is often interaction with ocean bottom. As the lower boundary, the ocean bottom is a multilayered structure composed of sediments, where acoustic energy can be reflected from the interface formed by the bottom and subbottom layers or transmitted and absorbed. At low grazing angles, wave guide phenomena become significant and the ocean bottom, covered with sediments of different physical characteristics, becomes effectively part of the wave guide. Depending on the frequency of the acoustic energy, there is a need to know the acoustically relevant physical properties of the sediments from a few centimeters to hundreds of meters below the water/sediment interface.

Underwater acousticians and civil engineers are continuously searching for practical and economical means of determining the physical parameters of the marine sediments for applications in environmental and geological research, engineering, and underwater acoustics. Over the past three decades much effort has been put into this field both theoretically and experimentally, to determine the physical properties of the marine sediments. Experimental and forward/inverse modeling techniques indicate that the acoustic wave field in the water column and seismo-acoustic wave field in the seafloor can be utilized for remote sensing of the physical characteristics of the marine sediments.

Sediment Structure as an Acoustic Medium

Much of the floor of the oceans is covered with a mixture of particles of sediments range in size from boulder, gravels, coarse and fine sand to silt and clay, including materials deposited from chemical and biological products of the ocean, all being saturated with sea water. Marine sediments are generally a combination of several components, most of them coming from the particles eroded from the land and the biological and chemical processes taking place in sea water. Most of the mineral particles found in shallow and deep-water areas, have been transported by runoff, wind, and ice and subsequently distributed by waves and currents.

After these particles have been formed, transported, and transferred, they are deposited to form

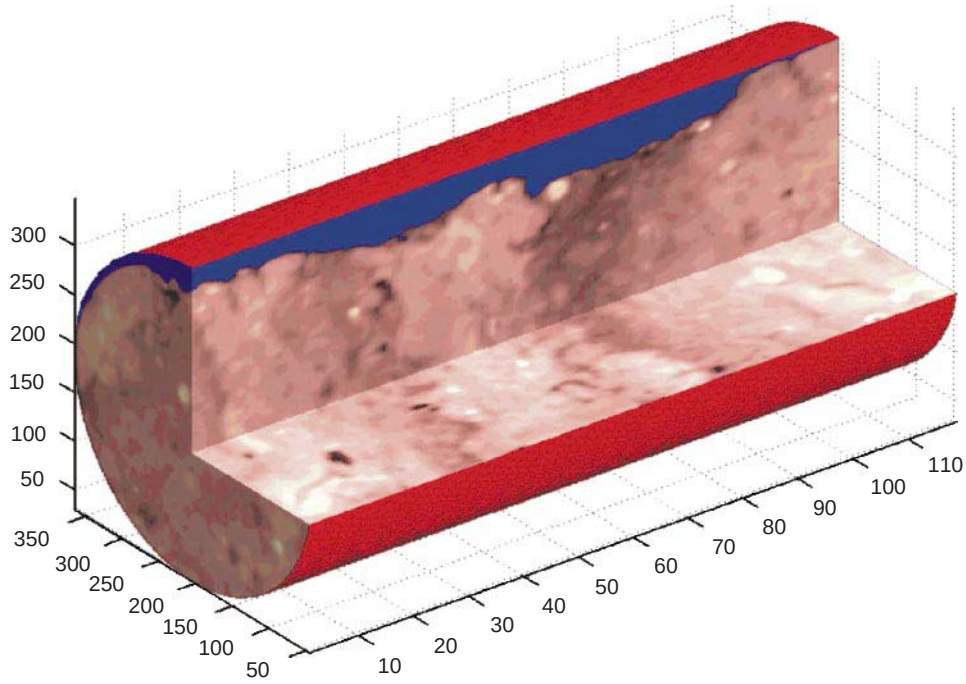

Figure 1 Three-dimensional reconstruction of a sediment core sample containing 75% sand, 15% silt and 10% clay. Scale in mm.

the marine sediments where the physical factors such as currents, dimensions and shapes of particles and deposition rate influence the spatial arrangements and especially sediment layering. Particles settle to the ocean floor and remain in place when physical forces are not sufficiently strong to move them. In areas with strong physical forces (tidal and ocean currents, surf zones etc.) large particles dominate, whereas in low motion energy areas (ocean basins, enclosed bays) small particles dominate.

During the sedimentation process these particles, based on the physical and chemical interparticle forces between them, form the sedimentary acoustic medium: larger particles (e.g., sands) by direct contact forces; small particles (e.g., clays and fine silts) by attractive electrochemical forces; and silts, remaining between sands and clays are formed by the combination of these two forces. The amount of the space between these particles is the result of different factors, mainly size, shape, mineral content and the packing of the particles determined by currents and the overburden pressure present on the ocean bottom.

Figure 1 is an example of a core taken very carefully by divers, to ensure an undisturbed internal structure of the sediment sample. Sediment structures have been quantified by using X-ray computed tomography to obtain values of density with a millimeter resolution for the full three-dimensional volume. The image shown in **Figure 1** is a false color 3D reconstruction of a core sample at a site where sediments consist of sandy silt (75% sand, 15% silt, and 10% clay) and shell pieces.

The results of the X-ray tomography of the same core, can also be shown on an X-ray cross-section slice along the center of the core (**Figure 2A**) and the corresponding two-dimensional spectral density levels for that cross-section (**Figure 2B**). The complex structure of the sediments can be seen with strong heterogeneity (local density fluctuation) of the medium that controls the interaction of the seismo-acoustic energy. In addition to the complex fine structure described above, the seafloor can also show complex layering (**Figure 3A**) or a simpler structure (**Figure 3B**). These structures result from the lowering of sea levels during the glaciation of the Pleistocene epoch during which sand was deposited over wide areas of the continental shelves. Unconsolidated sediments subsequently covered the shelves as the sea level rose in postglacial times.

Biot–Stoll Model

Various theories have been developed to describe the geoacoustic response of marine sediments. The most comprehensive theory is based on the Biot model as elaborated by Stoll. This model takes into account various loss mechanisms that affect the

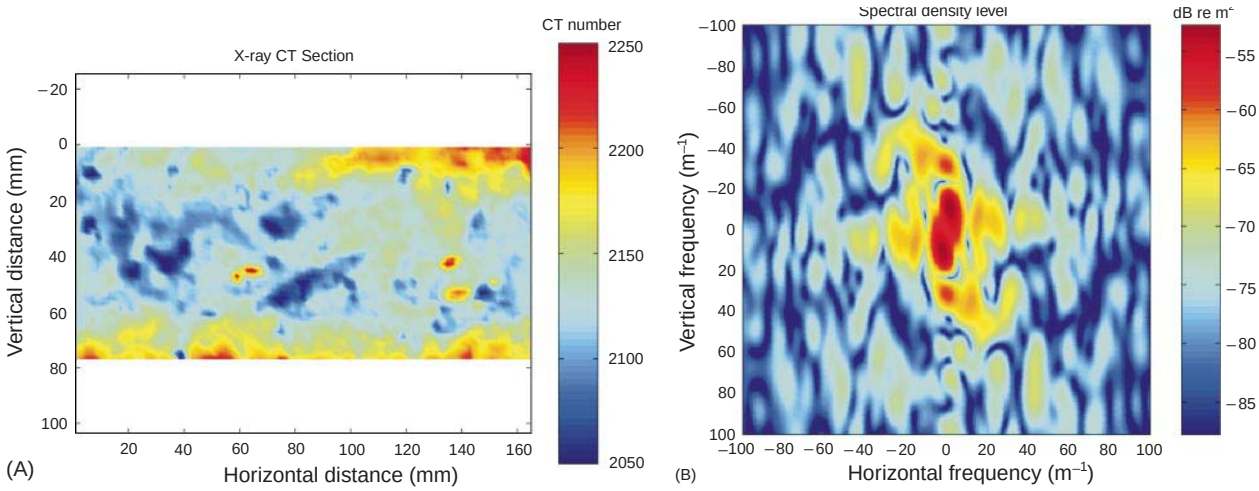

Figure 2 (A) X-ray cross-section slice along the center of the core shown in **Figure 1**. (B) 2-D spectral density levels for the cross-section shown in (A).

response of porous sediments that are saturated with fluid. The Biot–Stoll theory shows that acoustic wave velocity and attenuation in porous, fluid-saturated sediments depend on a number of parameters including porosity, mean grain size, permeability, and the properties of the skeletal frame.

According to the Biot–Stoll theory, in an unbounded, fluid-saturated porous medium, there are three types of body wave. Two of these are dilatational (compressional) and one is rotational (shear). One of the compressional waves ('first kind') and the shear wave are similar to body waves in an elastic medium. In a compressional wave of the 'first kind', the skeletal frame and the sea water filling the pore space move nearly in phase so that the attenuation due to viscous losses becomes relatively small. In contrast, due to out-of-phase movement of the frame and the pore fluid, the compressional wave of the 'second kind' becomes highly attenuated. The Biot theory and its extensions by Stoll have been used by many researchers for detailed description of the acoustic wave–sediment interaction when basic input parameters such as those shown in **Table 1** are available.

Seismo-acoustic Waves in the Vicinity of the Water–Sediment Interface

As mentioned above, when acoustic energy interacts with the seafloor, the energy creates two basic types of deformation: translational (compressional) and rotational (shear). Solution of the equations of the wave motion shows that each of these types of deformation travels outward from the source with its own velocity. Wave type, velocity, and propagation direction vary in accordance with the physical properties and dimensions of the medium.

The ability of seafloor sediments to support the seismo-acoustic energy depends on the elastic properties of the sediment, mainly the bulk modulus (incompressibility, K) and the shear modulus (rigidity, G). These parameters are related to the compressional and shear velocities C_P and C_S respectively, by:

$$C_P = [(K + 4G/3)/\rho]^{1/2}$$

$$C_S = (G/\rho)^{1/2}$$

where, ρ is the bulk density. **Table 2** shows basic seismic–acoustic wave types and their velocities related to elastic parameters.

These two types of deformations (compressional and shear) belong to a group of waves (body waves) that propagate in an unbounded homogeneous medium. However, in nature the seafloor is bounded and stratified with layers of different physical properties. Under these conditions, propagating energy undergoes characteristic conversions every time it interacts with an interface: propagation velocity, energy content, and spectral structure and propagation direction changes. In addition, other types of waves, i.e., ducted waves and surface waves, may be generated. These basic types of waves and their characteristics together with their arrival structure as synthetic seismograms for orthogonal directions are illustrated in **Figure 4**.

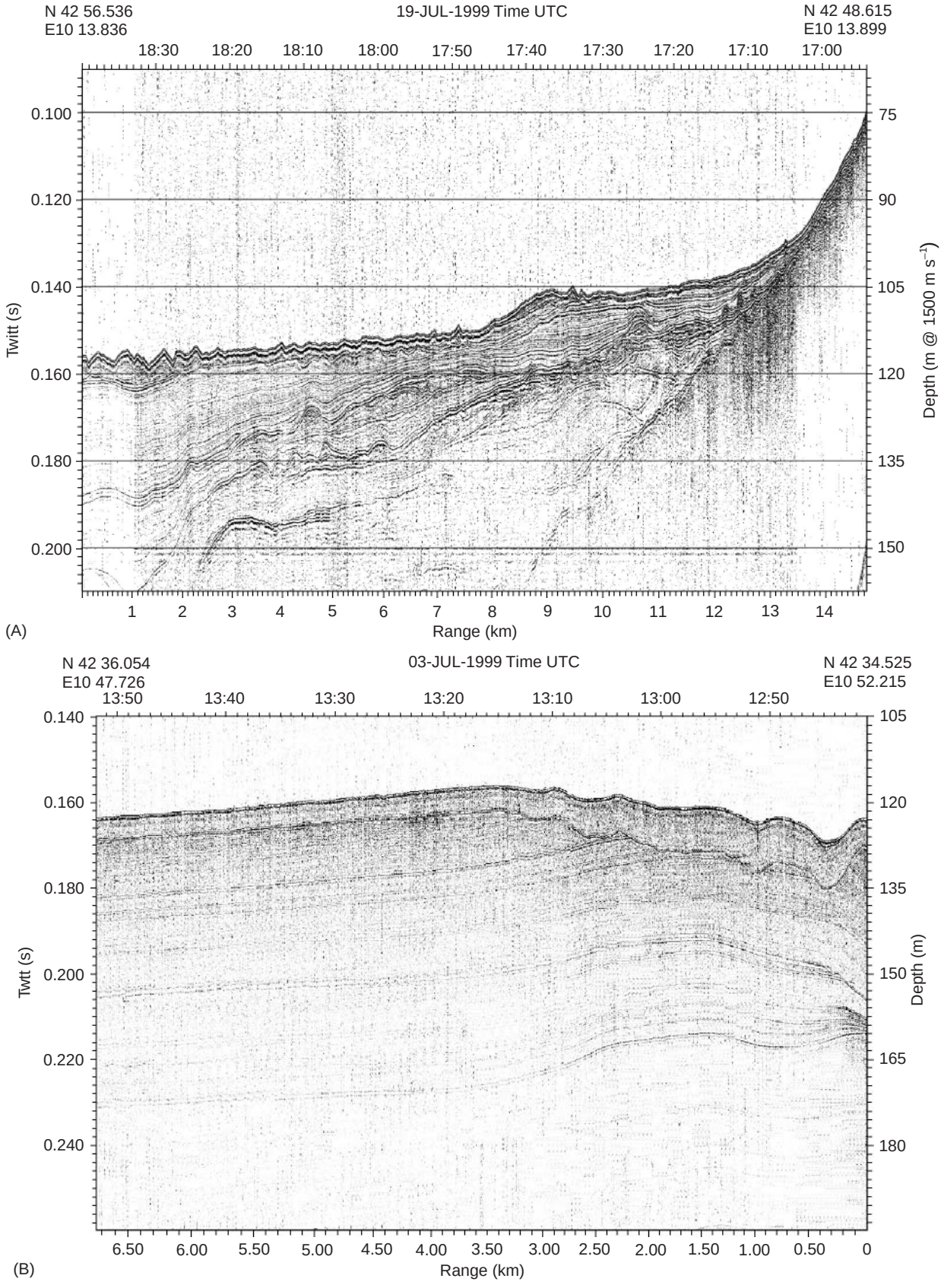

Figure 3 Seismic reflection profiles showing (A) complex and (B) simple structures of sediment layers.

Table 1 Basic input parameters to Biot–Stoll model

Frequency-independent Variables	
Porosity (%)	P
Mass density of grains	ρ_r
Mass density of pore fluid	ρ_f
Bulk modulus of sediment grains	K_r
Bulk modulus of pore fluid	K_f
Variables affecting global fluid motion	
Permeability	k
Viscosity of pore fluid	η
Pore-size parameter	a
Structure factor	α
Variables controlling frequency-dependent response of frame	
Shear modulus of skeletal frame	$\bar{\mu} = \mu_r(\omega) + i\mu_i(\omega)$
Bulk modulus of skeletal frame	$\bar{K}_b = K_{br}(\omega) + iK_{bi}(\omega)$

Body Waves

These waves propagate within the body of the material, as opposed to surface waves. External forces can distort solids in two different ways. The first involves the compression of the material without changing its shape; the second implies a change in shape without changing its volume (distortion). From earthquake seismology, these compressional and distortion waves are called primus (P) and 'secoundus' (S), respectively, for their arrival sequence on earthquake records. However, the distortional waves are very often called 'shear'.

Compressional waves Compressional waves involve compression of the material in such a manner that the particles move in the direction of propagation.

Shear waves Shear waves are those in which the particle motion is perpendicular to the direction of propagation. These waves can be generated at a layer interface by the incidence of compressional waves at other than normal incidence. Shear wave energy is polarized in the vertical or horizontal planes, resulting in vertically polarized shear waves (SV) and horizontally polarized shear waves (SH). However, if the interfaces are close (relative to a wavelength), one cannot distinguish between body and surface waves.

Ducted Waves

Love waves Love waves are seismic surface waves associated with layering; they are characterized by horizontal motion perpendicular to the direction of propagation (SH wave). These waves can be considered as ducted shear waves traveling within the duct of the upper sedimentary layer where total reflection occurs at the boundaries; thus the waves represent energy traveling by multiple reflections.

Interface Waves

Seismic interface waves travel along or near an interface. The existence of these waves demands the combined action of compressional and shear waves. Thus at least one of the media must be solid, whereas the other may be a solid (Stoneley wave), a liquid (Scholte wave), or a vacuum (Rayleigh wave). For two homogeneous half-spaces, interface waves are characterized by elliptical particle motion confined to the radial/vertical plane and by a constant velocity that is always smaller than the shear wave.

When different types of seismic waves propagate and interact with the layered sediments they are partly converted into each other and their coupling may create mixed wave types in the vicinity of the interface. **Figure 4** shows the basic seismo-acoustic

Table 2 Basic seismo-acoustic wave types and elastic parameters

Basic wave type		*Wave velocity*
Body wave	Compressional	$C_P = [(K + 4G/3)/\rho]^{1/2}$
	Shear	$C_S = (G/\rho)^{1/2}$
Ducted wave	Love	$C_L = (G/\rho)^{1/2}$
Surface wave	Scholte	$C_{SCH} = (G/\rho)^{1/2}$
Elastic parameters in terms of wave velocities (C) and bulk density (ρ)		
Bulk modulus (incompressibility)	$K = \rho(C_P^2 - 4C_S^2/3)$	
Compressibility	$\beta = 1/K$	
Young's modulus	$E = 2C_S^2\rho(1 + \sigma)$	
Poisson's ratio (transv./long. strain)	$\sigma = (3E - \rho C_P^2)/(3E + 2\rho C_P^2)$	
Shear modulus (rigidity)	$G = \rho C_S^2$	
Lame's constant	$\lambda = \rho(C_P^2 - 2C_S^2)$	

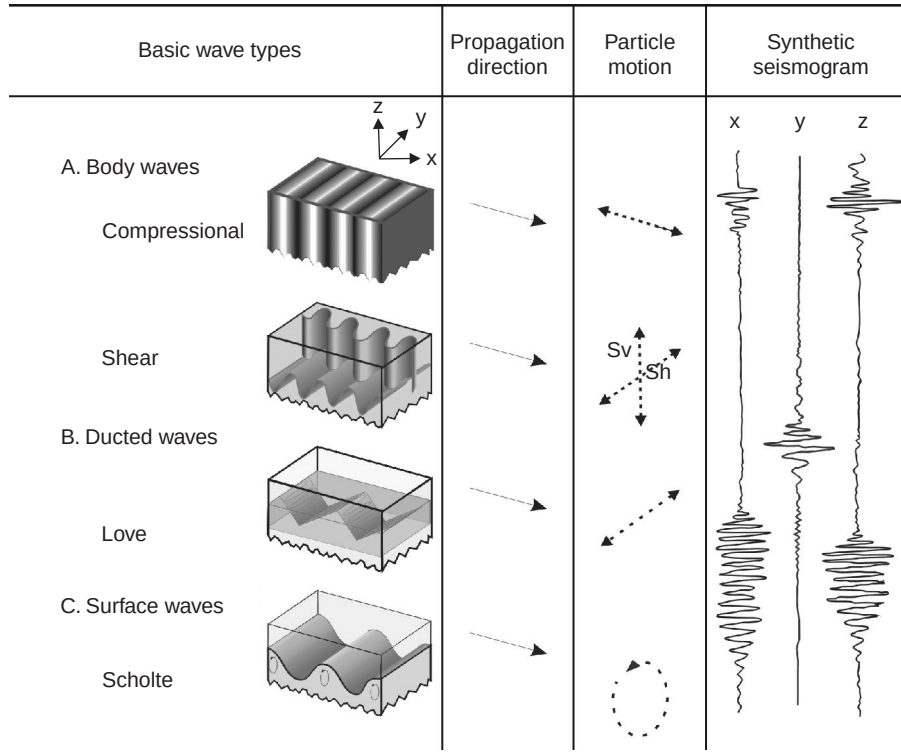

Figure 4 Basic seismo-acoustic waves in the vicinity of a water–sediment interface.

waves in the vicinity of a water/sediment interface. Basic characteristics of these waves together with their particle motion and synthetic seismograms at three orthogonal directions (x, y and z) are also illustrated in the same Figure. Under realistic conditions, in which the seafloor cannot be considered to be homogeneous, isotropic, nor a half-space, some of these waves become highly attenuated or travel together, making identification very difficult. In fact, the interface waves shown in **Figure 4** are for a layered seafloor, where the dispersion of the signal is evident (homogeneous half-space would not give any dispersion).

Under realistic conditions, i.e., for an inhomogeneous, bounded and anisotropic seafloor, some of these waves convert from one to another. The different wave types may travel with different speeds or together, and they generally have different attenuation. As an example, **Figure 5** shows signals from an explosive source (0.5 kg trinitrotoluene (TNT)) received by a hydrophone and three orthogonal geophones placed on the seafloor, at a distance of 1.5 km from the source. The broadband signal of a few milliseconds duration generated by the explosive source is dispersed over nearly 18 s demonstrating the arrival structure of different types of waves. The characteristics of these waves are indicated in the figure for four different sensors. They can be identified in order of their arrival time as: (a) head wave; (b) water arrival (compressional wave); (c) interface wave; (d) Love waves.

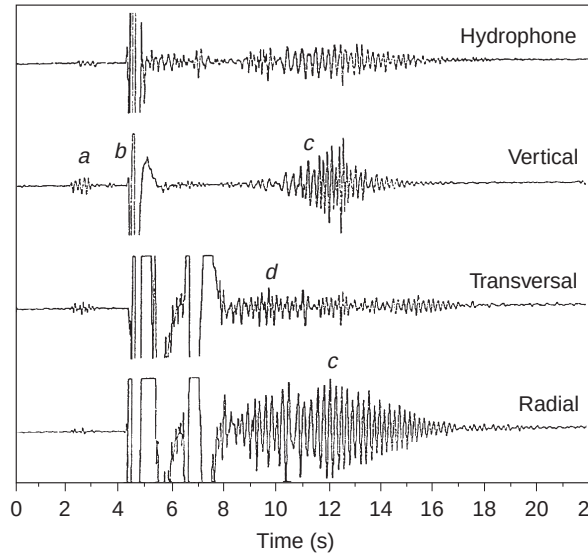

Figure 5 Signals from an explosive source of 0.5 kg trinitrotoluene received by a hydrophone and three orthogonal geophones at 1.5 km distance (a, Head wave; b, Compressional wave; c, Interface wave; d, Love wave).

Seafloor Roughness

The roughness of the water–sediment interface and layers below is another important parameter that needs to be considered in sediment acoustics. The seafloor contains a wide spectrum of topographic roughness, from features of the order of tens of kilometers, to those of the order of millimeters. The shape of the seafloor and its scattering effect on acoustic signals is covered here.

Techniques to Measure Geoacoustic Parameters of Marine Sediments

The geoacoustic properties of the seafloor defined by the compressional and shear wave velocities, their attenuation, together with the knowledge of the material bulk density, and their variation as a function of depth, are the main parameters needed to solve the acoustic wave equation. To be able to determine these properties of the seabed, different techniques have been developed using samples taken from the seafloor, instruments and divers conducting measurements *in situ*, and remote techniques measuring seismo-acoustic waves and inverting this information with realistic models into sediment properties. Some of the current methods of obtaining geoacoustic parameters of the marine sediments are briefly described here.

Laboratory Measurements on Sediment Core Samples

Most of our knowledge of the physical properties of sediments is acquired through core sampling. A large number of measurements on marine sediments have been made in the past. In undisturbed sediment core samples, under laboratory conditions, density and compressional velocity can be measured with accuracy, and having measured values of density and compressional velocity, the bulk modulus can be selected as the third parameter, where it can be calculated (**Table 1**).

There are several laboratory techniques available to measure some of the sediment properties. However, the reliability of such measurements can be degraded by sample disturbance and temperature and pressure changes. In particular, the acoustic properties are highly affected by the deterioration of the chemical and mechanical bindings caused by the differences in temperature and pressure between the sampling and the laboratory measurements. Controlling the relationships between various physical parameters can be used to check the accuracy of measured parameters of sediment properties. It has been shown that the density and porosity of sediments have a relationship with compressional velocity, and different empirical equations between them have been established.

Over the past three decades, at the NATO Undersea Research Centre (SACLANTCEN), a large number of laboratory and *in situ* measurements have been made of the physical properties of the seafloor sediments. These measurements have been conducted on the samples with the same techniques as when the same laboratory methods were applied. This data set with a great consistency of the hardware and measurement technique, has been used to demonstrate the physical characteristics of the sediment that affect acoustic waves.

The relationship between measured physical parameters From 300 available cores, 20 000 measured data samples for the density and porosity, and 10 000 samples for the compressional velocity were obtained. To be able to handle this large data set taken from different oceans at different water depths, all bulk density and compressional velocity data were converted into relative density (ρ) and relative velocity (C) with respect to the *in situ* water values:

$$\rho = \rho_S/\rho_W$$

$$C = C_S/C_W$$

where, ρ_S is sediment bulk density, ρ_W is water density, C_S is sediment compressional velocity and C_W is water compressional velocity. The data are not only from the water–sediment interface but cover sedimentary layers of up to 10 m deep.

Relative density and porosity The density and porosity of the marine sediment are least affected during coring and laboratory handling of the samples. Porosity is given by the percentage volume of the porous space and sediment bulk density by the weight of the sample per unit volume. The relationship between porosity and bulk density has been investigated by many authors with fewer data than used here and shown to have a strong linear correlation. Theoretically this linearity only exists if the dry densities of the mineral particles are the same for all marine sediments. The density of the sediment would then be the same as the density of the solid material at zero porosity, and the same as the density of the water at 100% porosity. **Figure 6** shows this relationship.

Porosity and relative compressional wave velocity The relationship between porosity and

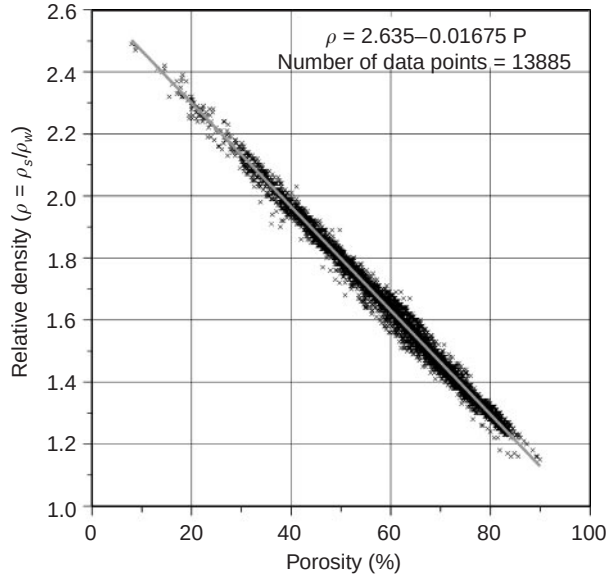

Figure 6 Relationship between relative density and porosity.

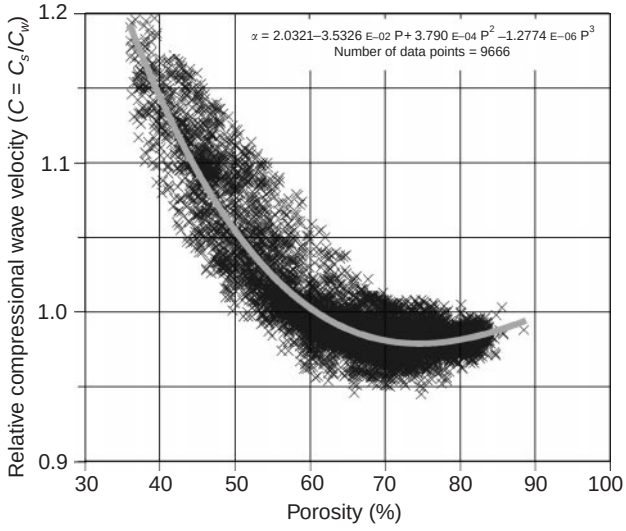

Figure 7 Relationship between relative compressional wave velocity and porosity.

compressional wave velocity has received much attention in the literature because porosity can be measured easily and accurately. Data from the SACLANTCEN sediment cores giving the relationship between porosity and compressional wave velocity are shown in **Figure 7**. As shown in **Figure 6** due to the linear relation between density and porosity, the relationship between density and compressional wave velocity is similar to the porosity compressional wave velocity relation.

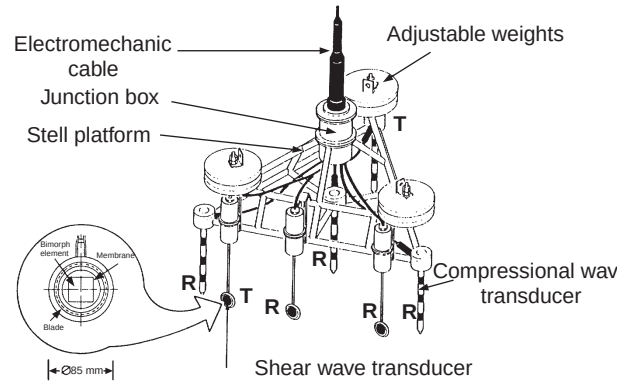

Figure 8 *In Situ* Sediment Acoustic Measurement System (ISSAMS) for near-surface *in situ* geoacoustic measurements.

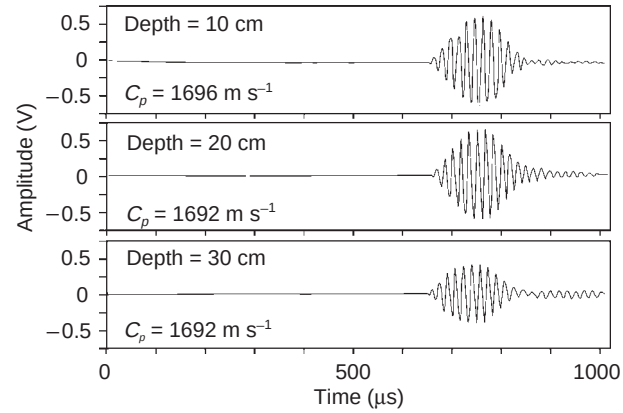

Figure 9 Examples of received compressional wave signals from fine sand sediment.

In situ Techniques

There are several *in situ* techniques available that use instruments lowered on to the seafloor mainly by means of submersibles, remotely operated vehicles (ROVs), and autonomous underwater vehicles (AUVs) and divers. The first deep-water, *in situ* measurements of sediment properties were made from the bathyscaph *Trieste* in 1962. These measurements provided accurate results due to the minimum disturbance of temperature and pressure changes compared to bringing the sample to the surface and for analysis in the laboratory. The most reliable direct geoacoustic measurement techniques for marine sediments are *in situ* techniques. Some of the approaches used in recent years are discussed below.

Near-surface method A system has been developed to measure sediment geoacoustic parameters, including compressional and shear wave velocities and

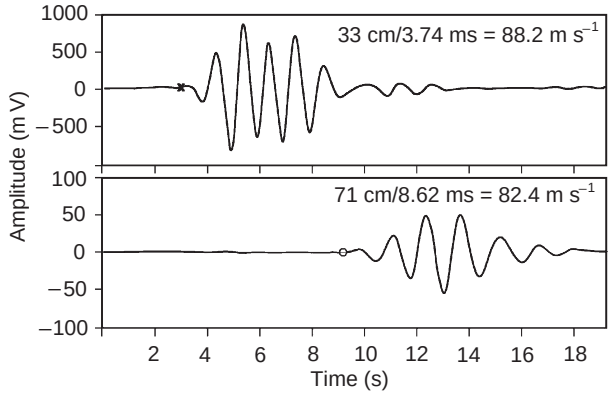

Figure 10 Examples of signals recorded from two shear wave receivers in hard-packed fine sand sediments.

their attenuation at tens of centimeters below the sediment–water interface. **Figure 8** shows the main features of the *In situ* Sediment Acoustic Measurement System (ISSAMS). Shear and compressional wave probes are attached to a triangular frame that uses weights to force the probes into the sediment. In very shallow water, divers can be used to insert the probes into the sediment, whereas in deeper water, a sleeve system (not shown) allows the ISSAMS to penetrate into the seafloor.

Using the compressional and shear wave transducers measurements are made with a continuous wave (cw) pulse technique where the ratio of measured transducer separation and pulse arrival time yields the wave velocity. Samples of compressional and shear wave data are shown in **Figures 9** and **10** respectively. **Table 3** gives a comparison of laboratory and *in situ* values of compressional and shear wave velocities from two different types of Adriatic Sea sediment.

Cross-hole method Measurements as a function of depth in sediments can be made with boreholes, using either single or cross-hole techniques. Boreholes are made by divers using water–air jets to penetrate thin-walled plastic tubes for cross-hole measurements. **Figure 11** shows the experimental set up for the cross-hole measurements. The source is in the form of an electromagnetic mallet securely coupled to the inner wall of one of the plastic tubes with a hydraulic clamping device.

With a separation range of 2.9 m, moving-coil geophone receivers are also coupled to the inner wall of the second plastic tube with a hydraulic clamping device. The electromagnetic mallet generates a point source on the thin plastic tube wall, which results in a multipolarized transient signal to the sediment. Depending on the orientation of receiving sensors, vector components of the propagating compressional and shear waves are received and analyzed for velocity and attenuation parameters. Examples of a time series and a frequency spectrum for a shear wave signal received by a geophone with a natural frequency of 4.5 Hz are shown in **Figure 12**.

Figure 13 shows shear wave velocity as a function of depth obtained in the Ligurian Sea. It can be seen that the shear wave velocities are around $60\,\mathrm{m\,s^{-1}}$ at the sediment interface and increase with depth.

Remote Sensing Techniques

Even though *in situ* techniques provide the most reliable data, they are usually more time consuming and expensive to make and they are limited to small areas. Remote sensing and inversion to obtain geoacoustic parameters can cover larger areas in less time and provide reliable information. These techniques are based on the use of a seismo-acoustic signal received by sensors on the seafloor and/or in the water column. **Figure 14** illustrates a characteristic shallow water signal from an explosion received by a hydrophone close to the sea bottom. Three different techniques to extract information relative to bottom parameters from these signals are described briefly below.

Reflected waves

The half-space seafloor. When the seafloor consists of soft unconsolidated sediments, due to its very low

Table 3 Comparison of laboratory and *in situ* measurements

			Wave velocity (ms^{-1})			
Sediment type	*Porosity* (%)	*Mean grain size* (ϕ)	*In situ* (C_P)	*Laboratory* (C_P)	*In situ* (C_S)	*Laboratory* (C_S)
Sand	37	3.5	1557–1568	1580–1604	78–82	50
Mud	68	8.6	1467–1488	1468–1487	27–31	15

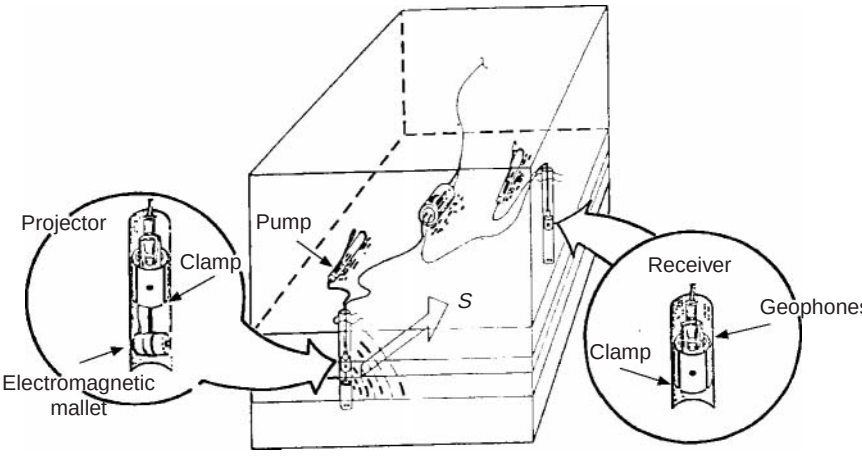

Figure 11 The experimental setup for cross-hole measurements.

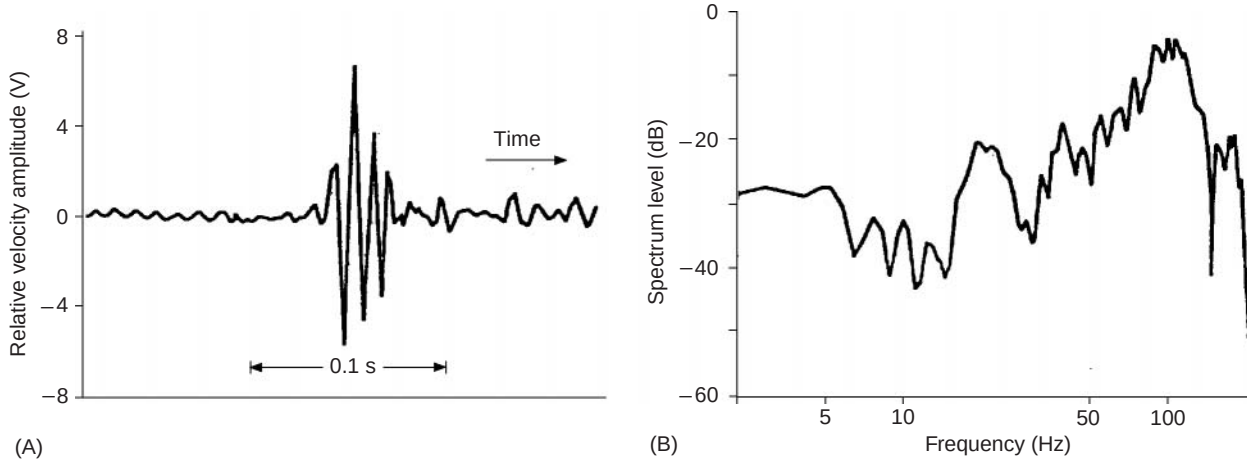

Figure 12 Cross-hole shear wave signal (A) and its spectrum (B) for a silty-clay bottom in the Ligurian Sea.

shear modulus it can be treated as fluid. Reflection may occur whenever an acoustic wave is incident on an interface between two media. The amount of energy reflected, and its phase relative to the incident wave, depend on the ratio between the physical properties on the opposite sides of the interface. It is possible to calculate frequency independent reflection loss as the ratio between the amplitude of the shock pulse and the peak of the first reflection (after correcting for phase shift, absorption in the water column, and differences in spreading loss). If the relative density $\rho = \rho_S/\rho_W$, and the relative compressional wave velocity $C = C_S/C_W$, are used to present the contrast between the two media, reflection coefficient for such a simple environmental condition can be written as:

$$R = \frac{\rho \sin\Theta - \sqrt{(1/C^2 - \cos^2\Theta)}}{\rho \sin\Theta + \sqrt{(1/C^2 - \cos^2\Theta)}}$$

where Θ is the grazing angle with respect to the interface as shown in **Figure 15**. For an incident path normal to a reflecting horizon, i.e., $\Theta = 90^\circ$, the reflection coefficient is:

$$R = \rho C - 1/\rho C + 1$$

Critical angle case. When the velocity of compressional wave velocity is greater in the sediment layer $(C > 1)$, as the grazing angle is decreased, a unique value is reached at which the acoustic energy totally reflects back to the water column. This is known as the critical angle and is given by:

$$\Theta_{cr} = \arccos(1/C)$$

When the grazing angle is less than this critical angle, all the incident acoustic energy is reflected. However, the phase of the reflected wave is then

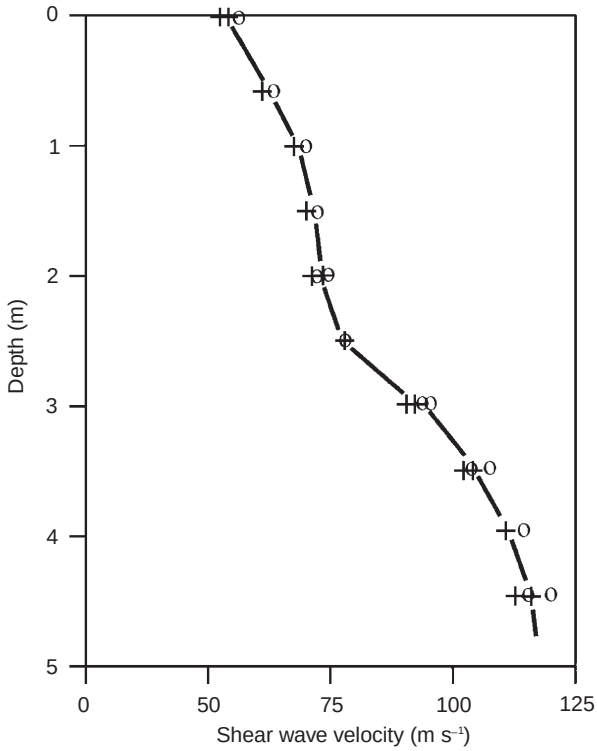

Figure 13 Shear wave velocity profile obtained from cross-hole measurements.

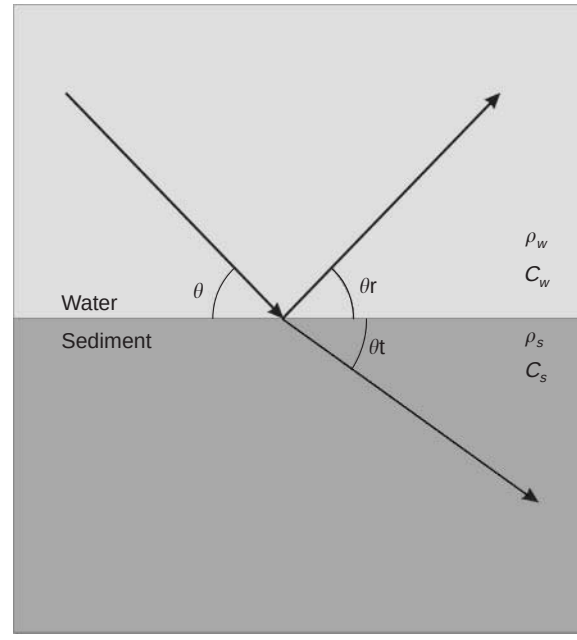

Figure 15 Geometry and notations for a simple half-space water–sediment interface.

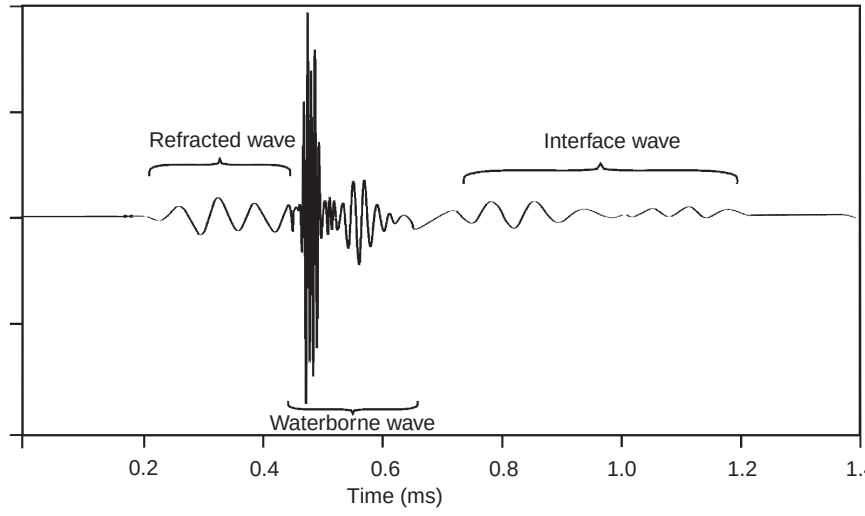

Figure 14 A characteristic shallow-water signal.

shifted relative to the phase of the incidence wave by an angle varying from 0° to 180° and is given as:

$$\Phi = -2\arctan\frac{\sqrt{(\cos^2\Theta - 1/C^2)}}{\rho\sin\Theta}$$

Figure 16(A) shows measured and calculated reflection losses (20 log R) for this simple condition together with the basic physical properties of the core sample taken in the same area for explosive signals at different grazing angles.

Angle of intromission case Especially in deep-water sediments the sound velocity in the top layer of the bottom is generally less than in the water above ($C < 1$). In such conditions there is an angle

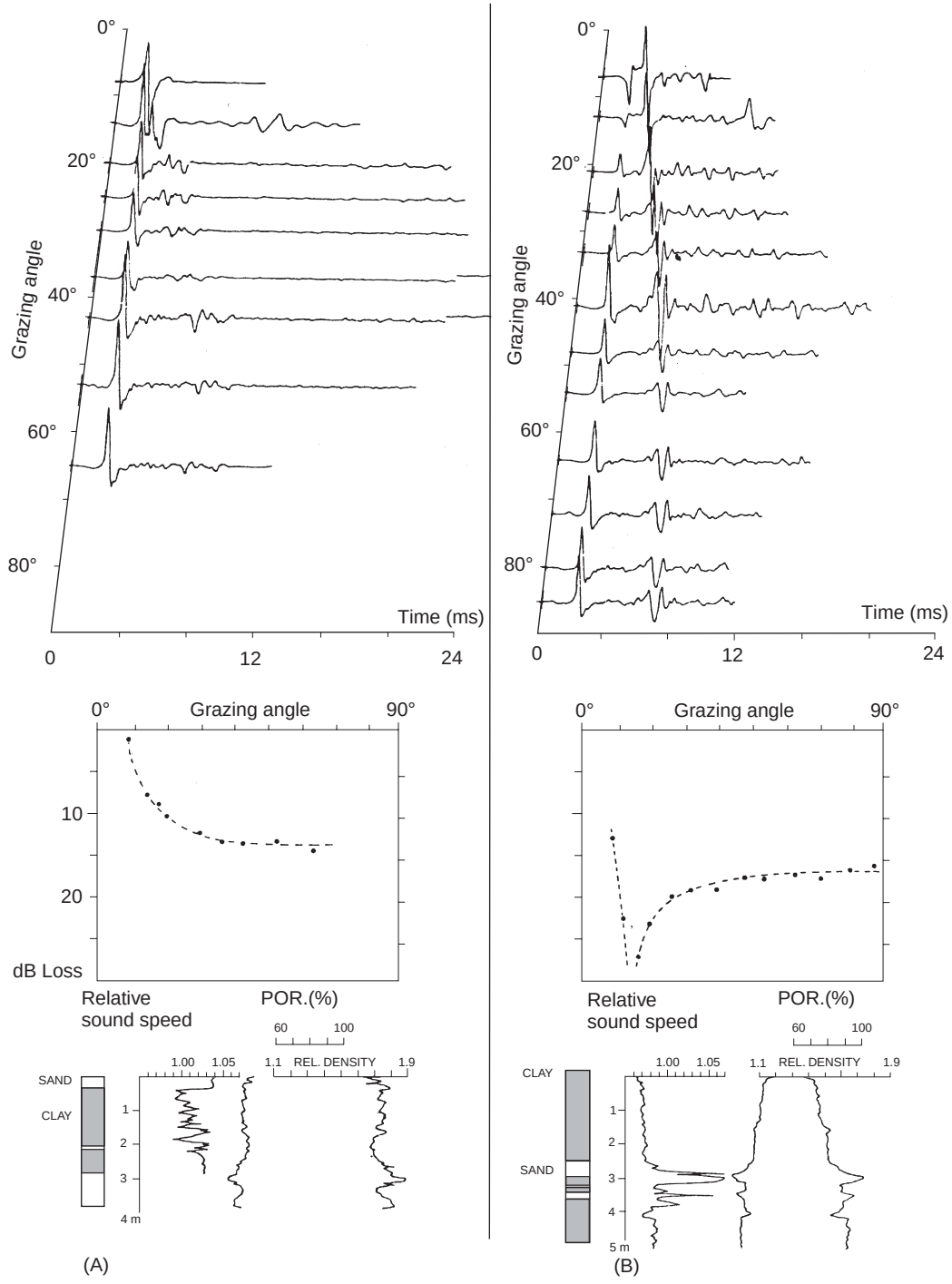

Figure 16 Acoustic signals and reflection loss as a function of grazing angle and sediment core properties: (A) for critical angle; (B) for angle of incidence case.

of incidence at which all of the incident energy is transmitted into the sedimentary layer and the reflection coefficient becomes zero:

$$\cos \Theta_i = \sqrt{\left(\frac{\rho^2 - 1/C^2}{\rho^2 - 1}\right)}$$

The phase shift is 0° when the ray angle is greater than the intromission angle and 180° when it is smaller. Thus, acoustical characteristics of the bottom, such as the critical angle, the angle of incidence, the phase shift, and the reflection coefficient, are primarily influenced by the relative density

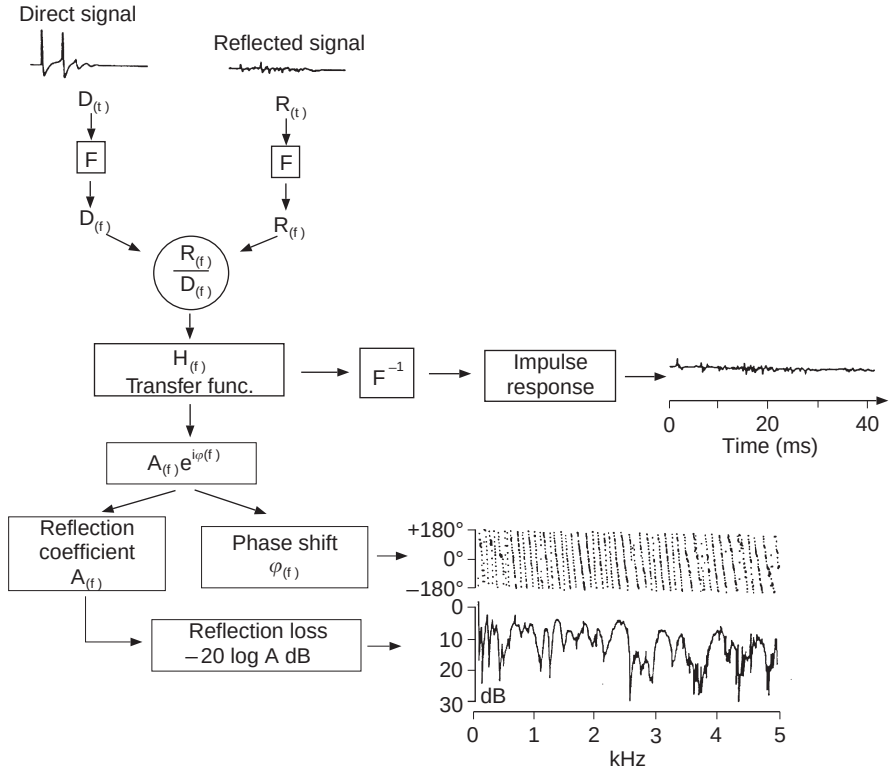

Figure 17 Acoustic reflection data and analysis technique for a layered seafloor.

and relative sound velocity of the environment as a function of the ray angle.

The layered seafloor Since the seafloor is generally layered, a simple peak amplitude approximation cannot be implemented because of the frequency dependence. In this case one calculates the transfer function (or reflection coefficient) from the convolution of the direct reference signal with the reflected signal. Examples of the phase shift and reflection loss as a function of frequency are shown in **Figure 17**. The reflectivity can also be described in the time domain by the impulse response, which is the inverse Fourier transform of the transfer function as shown in the same figure. This type of data can be utilized for inverse modeling to obtain the unknown parameters of the sediments. **Figure 18** is an example of measured and calculated reflection losses and impulse responses for a layered seafloor.

Refracted waves Techniques developed for remote sensing of the uppermost sediments (25–50 m below the seafloor) utilize broad-band sources (small explosives) and an array of geophones deployed on the seafloor. To obtain estimates of the bottom properties as a function of depth, both refracted compressional and shear waves as well as interface waves are analyzed. Inversion of the data is carried out using modified versions of techniques developed by earthquake seismologists to study dispersed Rayleigh-waves and refracted waves. **Figure 19** illustrates the basic experimental setup and **Figure 20** the signals received by an array of 24 geophones that permit studies of both interface and refracted waves.

These data are analyzed and inverted to obtain both compressional and shear wave velocities as a function of depth in the seafloor. Studies of attenuation and lateral variability are also possible using the same data set.

Figure 21 shows the expanded early portion of the geophone data shown in **Figure 20**, where the first arriving energy out to a range of about 250 m has been fitted with a curve showing that compressional waves refracted through the sediments just beneath the seafloor travel faster as they penetrate more deeply into the sediment. At zero offset, the slope indicates a velocity of $1505\,\mathrm{m\,s^{-1}}$ whereas at a range offset at 250 m the slope corresponds to a velocity of $1573\,\mathrm{m\,s^{-1}}$. At ranges over 250 m, a strong head wave becomes the first arrival and, the

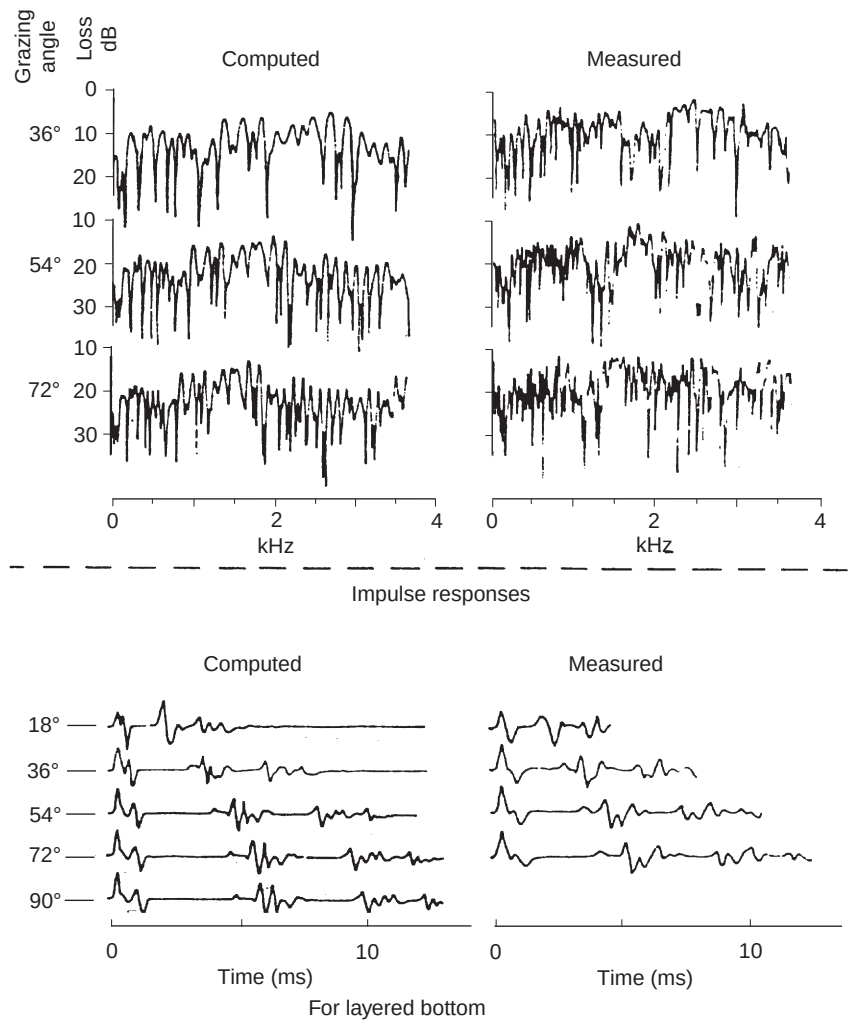

Figure 18 Measured and calculated reflection losses for a layered seafloor.

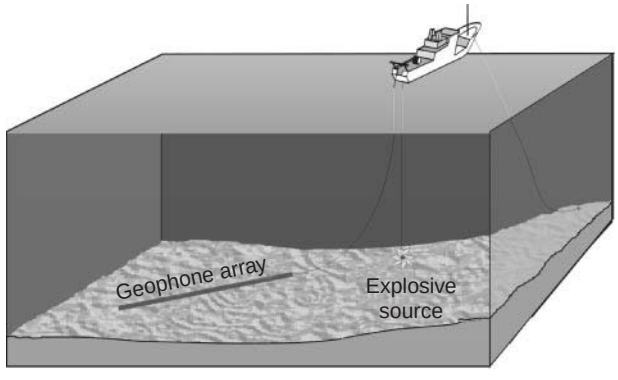

Figure 19 Experimental setup to measure seismo-acoustic waves on the seafloor.

interpretation would be that there is an underlying rock layer with compressional wave velocity of about $4577\,\mathrm{m\,s^{-1}}$.

A compressional wave velocity–depth curve for the upper part of the seafloor can be derived from the first arrivals shown in **Figure 21** using the classical Herglotz–Bateman–Wieckert integration method. The slope of the travel-time curve (fitted parabola) gives the rate of change of the range with respect to time that is also the velocity of propagation of the diving compressional wave at the level of its deepest penetration (turning point) into the sediment. At each range Δ, the depth corresponding to the deepest penetration is then calculated using the following integral

$$z(V) = 1/\pi \int_0^{\Delta} \cosh^{-1}(V(\mathrm{d}t/\mathrm{d}x))\mathrm{d}x$$

where

$$1/V = (\mathrm{d}t/\mathrm{d}x)_{x=\Delta}$$

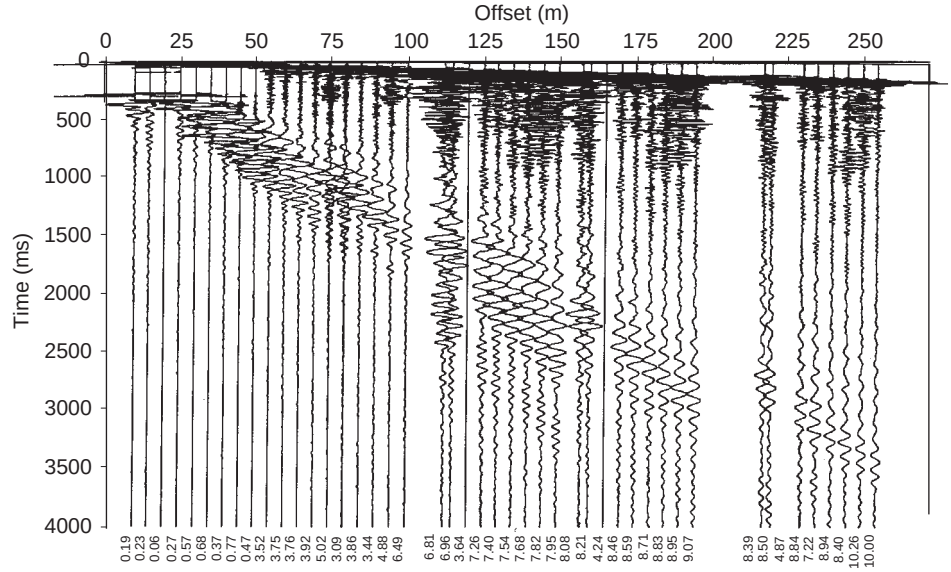

Figure 20 Signals received by geophone array.

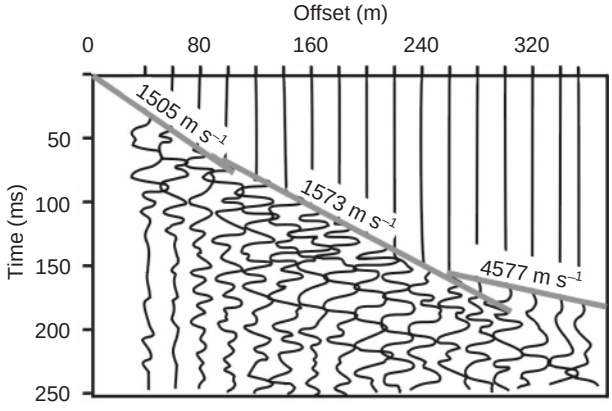

Figure 21 Expanded early portion of the data shown in **Figure 20**.

The result is the solid velocity–depth curve shown in **Figure 22**.

Interface waves In order to obtain a shear wave velocity–depth profile from the data, later arrivals corresponding to dispersed interface waves may be utilized (**Figure 20**). The portion of each individual signal corresponding to the interface-wave arrival can be processed using multiple filter analysis to create a group velocity dispersion diagram (Gabor diagram). The result of applying this technique to a dispersed signal is a filtered time signal whose envelope reaches a maximum at the group velocity arrival time for a selected frequency. The envelope is

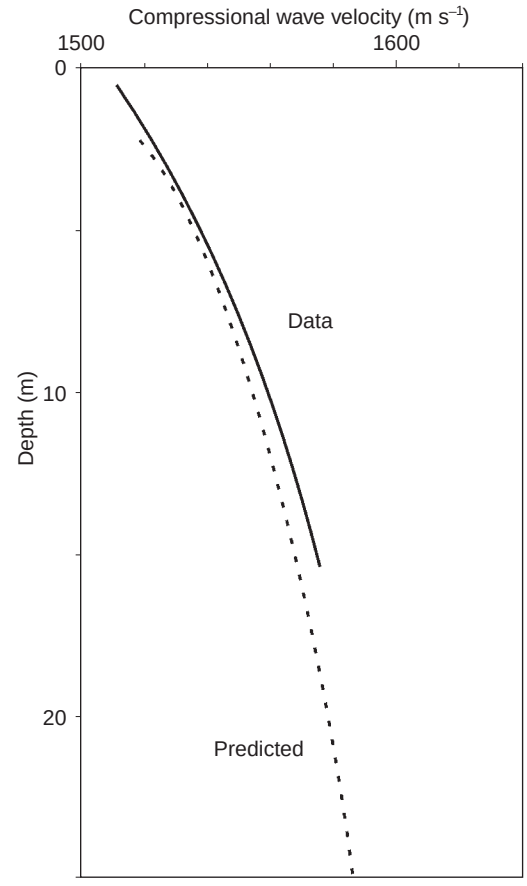

Figure 22 Compressional wave velocity versus depth curves derived from data and predicted (dashed line) by the model.

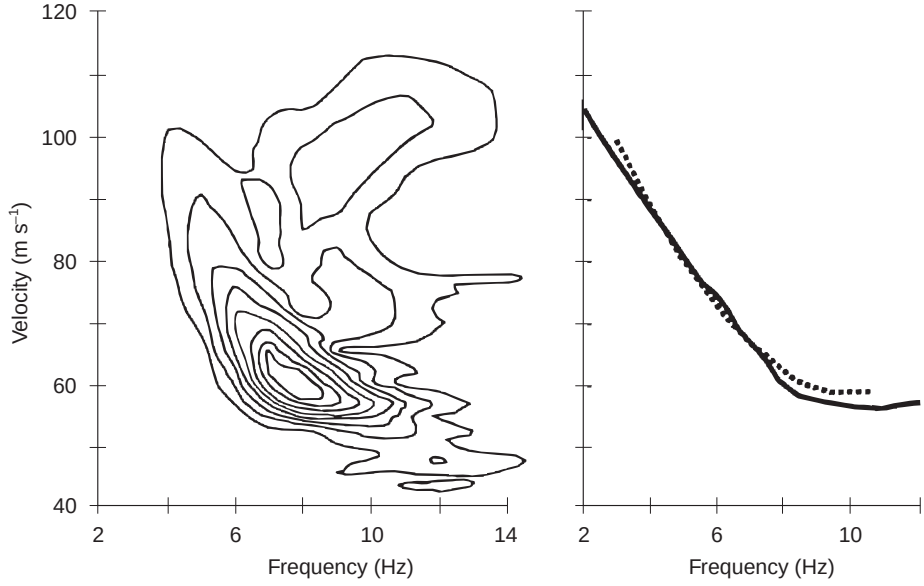

Figure 23 Dispersion diagram and measured and predicted dispersion curves.

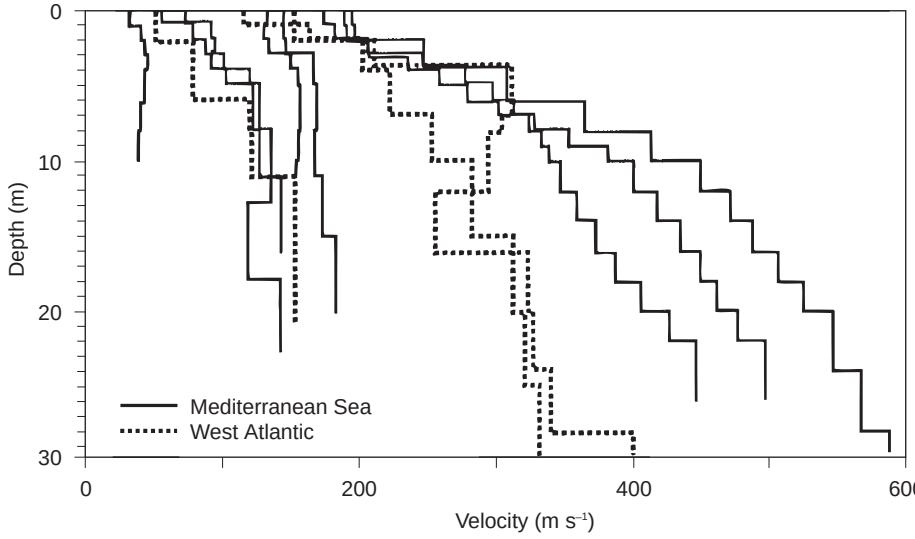

Figure 24 Summary of shear wave velocity profiles from the Mediterranean Sea.

computed by taking the quadrature components of the inverse Fourier transform of the filtered signal. Filtering is carried out at many discrete frequencies over selected frequency bands. Once the arrival times are converted into velocity, the envelopes are arranged in a matrix and contoured and dispersion curves are obtained by connecting the maximum values of the contour diagram (**Figure 23**).

Having obtained the dispersion characteristics of the interface waves, the geoacoustic model, made of a stack of homogeneous layers with different compressional and shear wave velocities for each layer that predict the measured dispersion curve is determined. **Figure 24** illustrates a number of examples from the Mediterranean sea covering data from soft clays to hard sands.

Transmission Loss Technique

The seafloor is known to be the controlling factor in low-frequency shallow water acoustic propagation. Forward modeling is performed with models giving exact solutions to the wave equation, i.e., SAFARI where, compressional and shear wave velocities, the attenuation factors associated with these waves, and the sediment density as a function of depth are the main input parameters. Acoustic energy propagating through a shallow water channel interacts with the

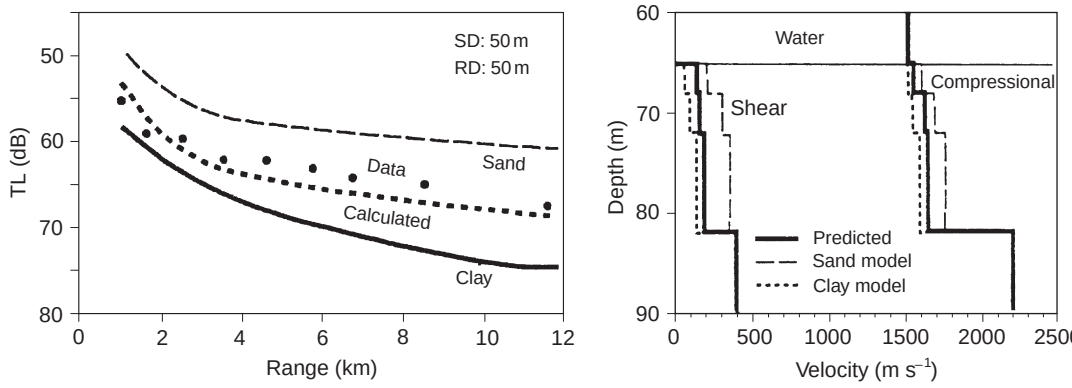

Figure 25 Comparison of transmission loss (TL) data and SAFARI prediction. Effects of changing bottom parameters from sand to clay is also shown together with the input profiles utilized for SAFARI predictions.

seafloor causing partitioning of waterborne energy into different types of seismic and acoustic waves. The propagation and attenuation of these waves observed in such an environment are strongly dependent on the physical characteristics of the sea bottom. Transmission loss (TL), representing the amount of energy lost along an acoustic propagation path, carries the information relative to the environment through which the wave is propagating. **Figure 25** shows a comparison of TL data and model predictions together with the input parameters used at 400 Hz. The effects of changes in bottom parameters are also shown in the figure. This technique becomes extremely useful when seafloor information is sparse.

Conclusions

Acoustic/seismic characteristics of the marine sediments have been of interest to a wide range of activities covering commercial operations involving trenching and cable lying, construction of offshore foundations, studies of slope stability, dredging and military applications like mine and submarine detection. Experimental and theoretical work over the years has shown that it is possible to determine the geoacoustic properties of sediments by different techniques. The characteristics of the marine sediments and techniques to obtain information about these characteristics have been briefly described. The studies so far conducted indicate that direct and indirect methods developed over the last four decades may give sufficient information to deduce some of the fundamental characteristics of the marine sediments. It is evident that still more research needs to be done to develop these techniques for fast and reliable results.

See also

Acoustics, Deep Ocean. Acoustics, Shallow Water. Benthic Boundary Layer Effects. Calcium Carbonates. Clay Mineralogy. Ocean Margin Sediments. Pore Water Chemistry. Seismic Structure.

Further Reading

Akal T and Berkson JM (ed.) (1986) *Ocean Seismo-Acoustics*. New York and London: Plenum Press.

Biot MA (1962) Generalized theory of acoustic propagation in porous dissipative media. *Journal of Acoustical Society of America* 34: 1254–1264.

Brekhovskikh LM (1980) *Waves in Layered Media*. New York: Academic Press.

Cagniard L (1962) *Reflection and Refraction of Progressive Seismic Waves*. New York: McGraw-Hill.

Grant FS and West GF (1965) *Interpretation and Theory in Applied Geophysics*. New York: McGraw Hill.

Hampton L (ed.) (1974) *Physics of Sound in Marine Sediments*. New York and London: Plenum Press.

Hovem JM, Richardson MD and Stoll RD (eds) (1992) *Shear Waves in Marine Sediments*. Dordrecht: Kluwer Academic.

Jensen FB, Kuperman WA, Porter MB and Schmidt H (1999) *Computational Ocean Acoustics*. New York: Springer-Verlag.

Kuperman WA and Jensen FB (eds) (1980) *Bottom Interacting Ocean Acoustics*. New York and London: Plenum Press.

Lara-Saenz A, Ranz-Guerra C and Carbo-Fite C (eds) (1987) *Acoustics and Ocean Bottom*. II F.A.S.E. Specialized Conference. Inst. De Acustica, Madrid.

Pace NG (ed.) (1983) *Acoustics and the Sea-Bed*. Bath: Bath University Press.

Pouliquen E, Lyons AP, Pace NG et al (2000) *Backscattering from unconsolidated sediments above 100 kHz*. In: Chevret P and Zakhario ME (ed) Proceedings of the fifth European Conference on Underwater Acoustics, ECUA 2000 Lyon, France.

Stoll RD (1989) *Lecture Notes in Earth Sciences: Sediment Acoustics*. New York: Springer-Verlag.